

CCD based phase resolved stroboscopic photometry of pulsars

Jurij Kotar, Simon Vidrih, Andrej Čadež

Department of Physics, Faculty of Mathematics and Physics, University of Ljubljana, Jadranska 19, 1000 Ljubljana, Slovenia

Abstract

A stroboscope designed to observe pulsars in the optical spectrum is presented. The absolute phase of the stroboscope is synchronized to better than $2.5\,\mu\text{s}$ with the known radio ephemerides for a given pulsar. The absolute timing is provided by the GPS clock. With such a device phase resolved photometry of pulsars can be performed. We demonstrate the instrument's capabilities with the results of a set of observations of the Crab pulsar, the brightest of the known optical pulsars, with a visual magnitude of 16.5, and a rotational frequency of $\sim 29\,\text{Hz}$.

1. Introduction

In this paper we present an improved version of the stroboscopic system, previously developed and used for observing faint optical signals from pulsars, specifically the signal from the Crab pulsar^{1–3}. Pulsars are fast rotating neutron stars⁴. Relativistic processes in the pulsar magnetosphere give rise to synchrotron emission, which is subsequently modulated by the neutron star's rotation. This results in a periodic train of pulses, the latter typically being a small fraction of the pulsar's rotation period. For pulsars the rotation periods range from several milliseconds to several seconds.

The main idea of the stroboscopic system is to observe the light signal periodically only during part of the period. The technique is based on a shutter that opens with the prescribed frequency and phase. In our case the shutter is a rotating wheel with out-cuts whose width determines the fraction of the period during which a light detector - in this case a CCD camera - is illuminated. Photometry is usually performed with a chopper with out-cuts corresponding to the pulse width and with the phase of the chopper synchronized to the topocentric pulse arrival times of a given pulsar.

The commonly applied method for observing pulsars at optical wavelengths is by high-speed photometers^{5–8}. This choice is dictated by the required time resolution. Normal CCDs are too slow for the task, since their typical integration times are several seconds, which may be more than hundreds of pulsar periods. However, we argue that a precisely timed stroboscope in front of a CCD camera can make up for the lack of time resolution and offers the advantage of the higher quantum efficiency⁹ as well as that of a more detailed field of view. It thus enables highly accurate phase resolved photometry of even fast pulsars. We note, however, that in the last years the time resolution of CCDs has been increased by the use of frame transfer technique, so that second¹⁰ and even subsecond¹¹ resolution has been achieved. An ingenious method of periodically saving (linear) spectroscopic data by a CCD

has been applied and used by Fordham et al.^{12,13}.

2. Principle of operation

From the observer's point of view the frequency of a pulsar is constantly changing due to the Doppler shift caused by the Earth's relative motion, the pulsar's spin down, and also due to changes in the local gravitational redshift. In the case of the Crab pulsar the maximal change of the frequency due to the Doppler shift is $\sim \pm 5 \times 10^{-5}$ Hz, while the first derivative of the frequency due to the pulsar spin down is $\sim -10^{-14}$ s $^{-2}$. All these effects are calculated with very high accuracy. Using the standard program TEMPO¹⁴ we calculate topocentric arrival times of pulses using known radio pulsar ephemerides and geographic coordinates of the observatory. Absolute timing provided by the GPS clock assures an accurate reference to the absolute radio phase of the pulsar.

The electronic system described in the next section drives the chopper so that it is phase locked with a given pulsar's ephemerides, which are derived from continual radio timing studies¹⁵. Thus one can examine the relation between the radio and the optical phase of the pulsar, search for other unknown periodic changes of the pulsar signal on a time scale longer than the integration time of a CCD¹⁶. One can also change the chopper phase in prescribed steps and thus investigate the shape of the pulse signal. Examples of such measurements together with stability tests are presented later in the paper.

3. Instrument

As shown in Figure 1, the system consists of a chopper, electronics for driving and controlling the chopper and a PC, connected via a serial port to the electronics.

The chopper is made of a steel blade 240 mm in diameter which has four out-cuts (Figure 2). The chopper blade is enclosed in a case and rotated by a stepper motor with 500 steps/revolution. When observing the Crab pulsar, it spins with one quarter of the Crab pulsar frequency which is approximately 7.5 Hz. The width of out-cuts is 9 degrees, which corresponds to the width of the Crab pulsar main pulse (see Figure 3). During observations the chopper is mounted in front of a CCD camera on a telescope. Optical sensors on the chopper housing are used to measure the phase of the blade once per revolution.

The electronics consists of the Truetime GPS receiver, model XL-DC 151-600-110¹⁷ and a set of proprietary electronics components (home made DDS board, stepper motor driver and microprocessor board).

A GPS receiver generates a highly accurate clock of $10(1 \pm 3 \times 10^{-12})$ MHz, which is used as a frequency reference. Two other functions of the receiver are used to: i) generation of short pulses at specified absolute time (used for frequency and phase control of the chopper blade) with an accuracy of 150 ns, and ii) the absolute measurement of arrival times of externally applied input signals which are generated by optical sensors on the chopper.

The DDS board is based on Analog Devices' AD9854 digital synthesizer¹⁸ which provides 48-bit frequency resolution. It generates clock output with resolution of 3.55×10^{-8} Hz from 10 MHz frequency reference. The clock output drives the stepper motor by means of two National Semiconductor's LMD18245 stepper motor driver chips¹⁹. The microcontroller

board based on Atmel AVR8515 microcontroller²⁰ is responsible for communication between DDS board, stepper driver, GPS receiver and the PC.

The system is controlled from the PC. First ephemerides for the pulsar phase are calculated by TEMPO and loaded in a control program which first sets the chopper to run with the frequency suitable for the starting time. Next the phase of the chopper with respect to the pulsar ephemerides is measured and calculated. This is done by repeatedly reading the GPS clock when the chopper out-cut passes the beam of light between a LED and a photodiode mounted on the enclosure (see Figure 2). After the absolute phase of the chopper has been established, the correction to the desired phase is calculated and the chopper driving is taken over by the computer to follow the phase, according to the output of the TEMPO program.

Here we should like to emphasize that our system relies on pulsar ephemerides, so that all accuracy measurements presented here are with respect to the ephemerides phase. In practice radio ephemerides for pulsars is not always very accurate. For example the Jodrell Bank ephemerides for the Crab pulsar is known to have an absolute phase uncertainty between 40 and 1000 microseconds. The relation between the radio and optical phase has not been extensively studied. However, from our (albeit limited) experience we can state: using Jodrell Bank ephemerides that is no older than 1/2 month and carefully measuring the phase with respect to the ephemerides on the first day, we find that during the next day of observations the peak brightness is obtained at the same relative phase.

The phase tracking accuracy depends on two circumstances: i) on the accuracy of the absolute phase ψ of the chopper with respect to the housing and ii) on the position of the beam from the pulsar with respect to the housing. The accuracy of the absolute phase is limited by timing noise, which we define as the difference between the time when the chopper actually opens and the time when it is expected to open. We measured the spectrum of this noise and found that it is mainly due to random excitations of mechanical resonances in the motor-chopper system (see Figure 4). Its RMS value was found to be $2.5\ \mu\text{s}$. The phase dependence ($\delta\psi$) on the position of the pulsar (position of the pulsar's image on the CCD) with respect to direction of the optical axis of the telescope ($\delta\phi$) is easily calculated from the geometry of the beam and is:

$$\delta\psi = \frac{4F}{r}\delta\phi \quad , \quad (1)$$

where F is the effective focal length of the telescope and r is the radius of the chopper. For the optical setup in Cananea this turns into $\delta\psi \approx 0.0054 \frac{\text{rad}}{\text{arcsec}} \delta\phi$. In order to avoid possible phase modulation by the periodic error in the telescope tracking, the chopper blade is mounted so as to cut into the beam in the north-south direction.

The phase guiding routine works as follows: the position angle of the chopper (ψ_i) at setting moments (t_i)²¹ is calculated as the sum of the initial phase and the phase increment, which is the integral of frequency corrections (DDS is particularly suitable for the task, because it is built in such a way that the result of integration is exact). The phase in the following moment (t_{i+1}) is calculated from TEMPO and the frequency necessary to reach this phase is calculated and set. The phase guiding routine is checked at will by additional measurement of the blade phase with GPS timing as described above. We thus verified in many hours of running that the phase guiding routine preserves the average (40 successive measurements) phase of the blade to within $0.5\ \mu\text{s}$ for several hours.

4. Experimental results

The stroboscopic system has been successfully tested during observations of the Crab pulsar at the 2.12 m telescope of the Guillermo Haro observatory in Cananea²² in January 2002. Since the Crab pulsar light curve is well known from other observations^{3,13,23}, one of the tests was to measure the light curve again and compare it with those previously obtained.

All the images were obtained with the EEV P8603 CCD detector and no filters. Thus the optical range of observation is approximately between 500 and 900 nm. During the observations biases and dome flats were taken in order to correct for the CCD bias and gain imperfections. The fluxes were calibrated with respect to the photometric standards PG 0942-029 and PG 1047+003 (Landolt²⁴). Note, however, that images were taken without filters, so the calibration is only relative.

The light curve was measured during the early night hours of January 9/10 2002. Sky conditions were changing with some scattered clouds in the sky. We covered the whole phase light curve with the set of 36 images $1/36 \times 2\pi$ apart in phase. The exposure time of each image was 45 seconds. The pulsar was detected in 18 frames and was too faint in the remaining 18 images. The results, shown as crosses in Figure 5 (the width is much larger than the actual phase uncertainty), agree with other measurements of the optical light curve^{13,23}. The solid curve in this Figure shows the optical light curve obtained by Fordham et al.¹³ convolved with our stroboscopic window function. We fitted our stroboscopic data to this curve allowing the phase difference and the flux scaling parameter to be determined by the fit. In this way we obtained²⁵ $\chi^2/(N - M) = \frac{140}{16}$. The χ^2 has been calculated assuming that the only noise is in our data and has the uncertainty given by IRAF/DAOPHOT^{26,27}, which is the uncertainty due to photon shot noise only. The additional systematic error in determining the flux from the pulsar which comes from its position in the middle of the nebula and from the neighboring comparably bright star has not been included in the calculation of χ^2 . By examining the data, we verified that the magnitude of the neighboring star is anti-correlated with that of the pulsar, making the variations of its flux about 2.5 times greater than the IRAF/DAOPHOT calculated value. Thus we conclude that our data agree with Fordham et al.¹³. Note that the amplitude of the systematic error discussed above is proportional to the ratio of maximum to minimum pulsar flux in the set of measurements, so that it becomes negligible for fixed phase photometry.

5. Acknowledgments

We are grateful to Alberto Carramiñana who made observations of the Crab pulsar possible and to Carramiñana, Fordham et al. who gave us data on the Crab pulsar phase light curve (see Figure 3) before publication. We thank the technical staff of the Cananea Observatory for friendly atmosphere and expert mounting of the instrument. Igor Poberaj gave the DDS board he developed. We thank Dick Manchester and David Nice for help with TEMPO. Dušan Babič criticized the text and made it more readable. We would also like to thank the anonymous referee whose comments and suggestions improved the presentation of this paper. This research was supported in part by the Ministry of Education Science and Sport of the Republic of Slovenia.

REFERENCES

1. A. Čadež and M. Galičič, *A&A*, **306**, 443 (1996)
2. A. Čadež, M. Galičič and M. Calvani, *A&A*, **324**, 1005 (1997)
3. M. Galičič, Observations of Minute Time-Scales Modulation of Pulsar PSR 0531+21 Optical Pulses, Ph. D. Thesis, (University of Ljubljana, 1999)
4. A. G. Lyne and F. G. Smith, *Pulsar Astronomy*, (Cambridge University Press, 1998)
5. D. Chakrabarty and V. M. Kaspi, *ApJ*, **498**, 37 (1998)
6. A. Golden, A. Shearer and G.M. Beskin, *ApJ*, **535**, 373 (2000)
7. A. Golden, A. Shearer, R.M. Redfern, G. M. Beskin, S. I. Neizvestny, V. V. Neustroev, V. L. Plokhotnichenko and M. Cullum, *A&A*, **363**, 617 (2000)
8. A. Golden, R. F. Butler and A. Shearer, *A&A*, **371**, 198 (2001)
9. The quantum efficiency of newly developed Avalanche Photodiodes is comparable with the quantum efficiency of a CCD²⁸.
10. V. Dhillon and T. Marsh, *NewAR*, **45**, 91 (2001)
11. B. Kern and C. Martin, *Nature*, **417** 527 (2002)
12. J. L. A. Fordham, H. Kawakami, R. M. Michel, R. Much and J. R. Robinson, *MNRAS*, **319**, 414 (2000)
13. J. L. Fordham, N. Vranesovic, A. Carramiñana, R. Michel, R. Much, P. Wehinger, S. Wyckoff, *ApJ* accepted
14. <http://pulsar.princeton.edu/tempo/>
15. Radio ephemerides of the Crab pulsar are available at the internet site of the Jodrell Bank Observatory (<http://www.jb.man.ac.uk/>)
16. A. Čadež, S. Vidrih, M. Galičič and A. Carramiñana, *A&A*, **366**, 930 (2001)
17. <http://www.truetime.com>
18. <http://www.analog.com>
19. <http://www.national.com>
20. <http://www.atmel.com>
21. Setting moments are started by GPS periodically at $t_i = i\Delta T$, where ΔT is usually a prime number of seconds.
22. <http://www.inaoep.mx/~astrofi/cananea/>
23. Percival et al., *ApJ*, **407**, 276 (1993)
24. A. U. Landolt, *AJ*, **104**, 340L (1992)
25. W. H. Press, S. A. Teukolsky, W. T. Vetterling, B. P. Flannery, *Numerical Recipes in C*, 2nd ed. (Cambridge University Press, 1992), p. 660
26. IRAF is the Image Reduction and Analysis Facility, a general purpose software system for the reduction and analysis of astronomical data. It is distributed by the National Optical Astronomy Observatories, which are operated by the Association of Universities for Research in Astronomy, Inc., under cooperative agreement with the National Science Foundation(<http://iraf.noao.edu/>).
27. DAOPHOT is a software package for doing stellar photometry in crowded fields developed by Peter Stetson²⁹. The IRAF/DAOPHOT package uses the task structure and algorithms of DAOPHOT to do crowded field photometry within the IRAF data reduction and analysis environment.
28. C. Straubmeier, G. Kanbach and F. Schrey, *ExA*, **11**, Issue 3, 157 (2001)
29. P. B. Stetson, *PASP*, **99**, 191 (1987)

FIGURES

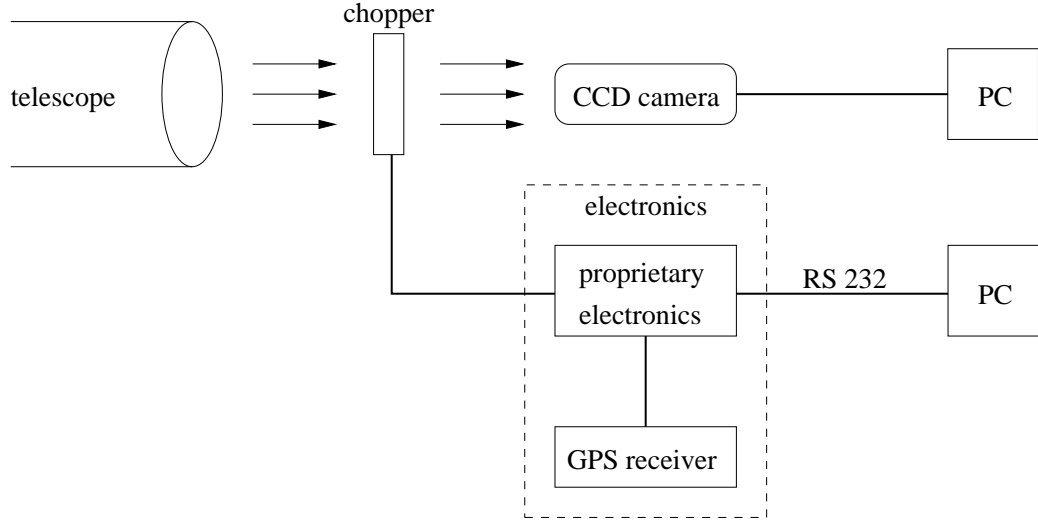


Fig. 1. The sketch of the stroboscopic system. The CCD camera is independently connected to another PC.

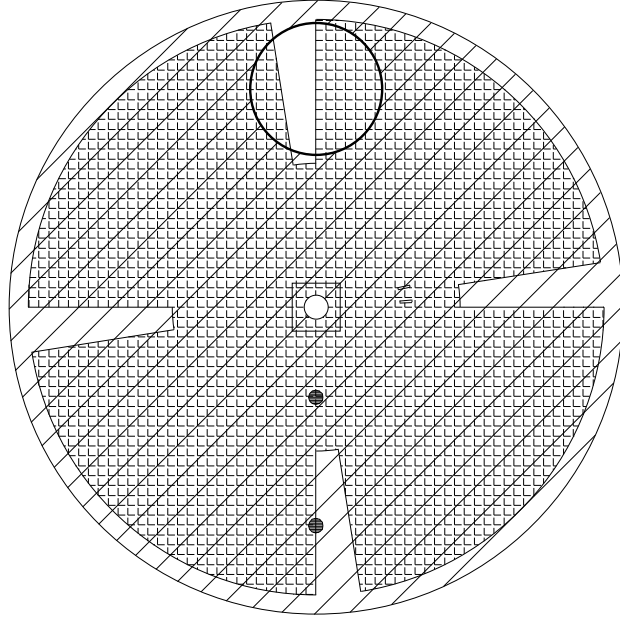


Fig. 2. The drawing of the chopper. The light passing through the hole in the enclosure is chopped with the rotating blades. Optical sensors on the enclosure (marked as two black spots) measure the position of the blade once per revolution.

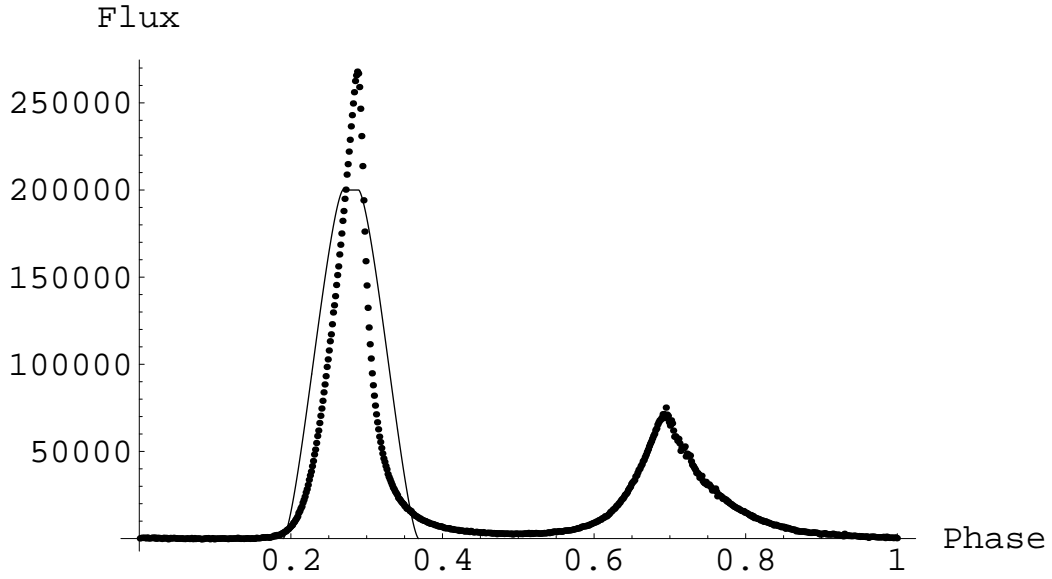


Fig. 3. The light curve of the Crab pulsar, obtained by Fordham et. al ¹³. The width of the main pulse is $\sim 10\%$ of the whole period. The stroboscopic window function is also displayed and has been calculated on the basis of the width of the chopper blade out-cut and the position of the chopper blade with respect to the focal plane of the telescope.

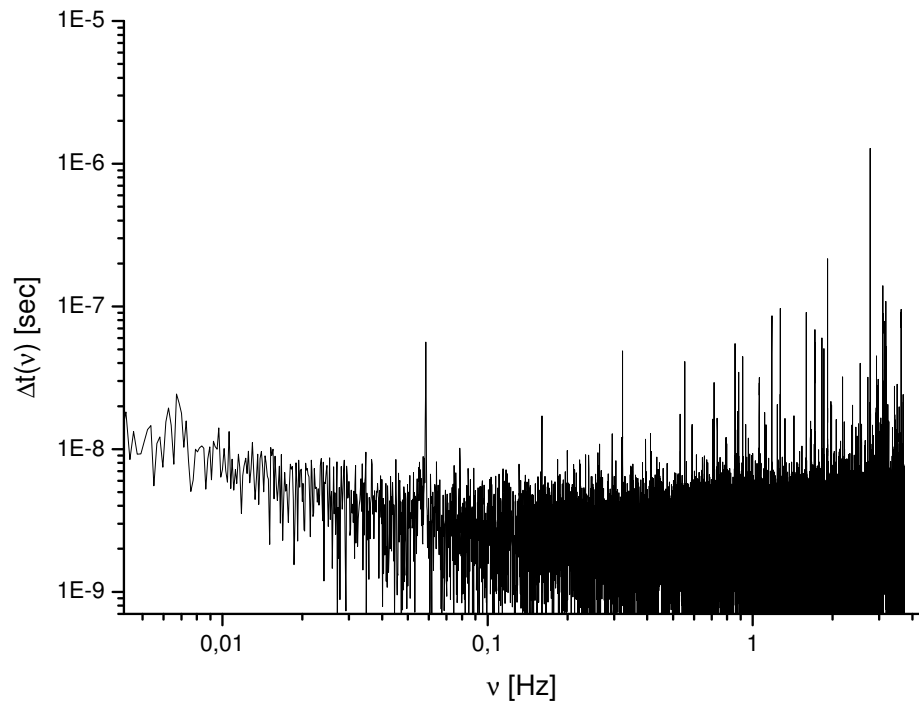


Fig. 4. Frequency spectrum of timing noise. $\delta t(t_i) = [\int_0^{t'_i} \nu(t)dt - i]/\nu(t'_i)$, where t'_i is the time of detecting the i -th passage of the chopper through the LED trigger and $\Delta t(\nu)$ is the Fourier transform $\frac{1}{T} \int_0^T \delta t(x) e^{-2\pi i \nu x} dx$.

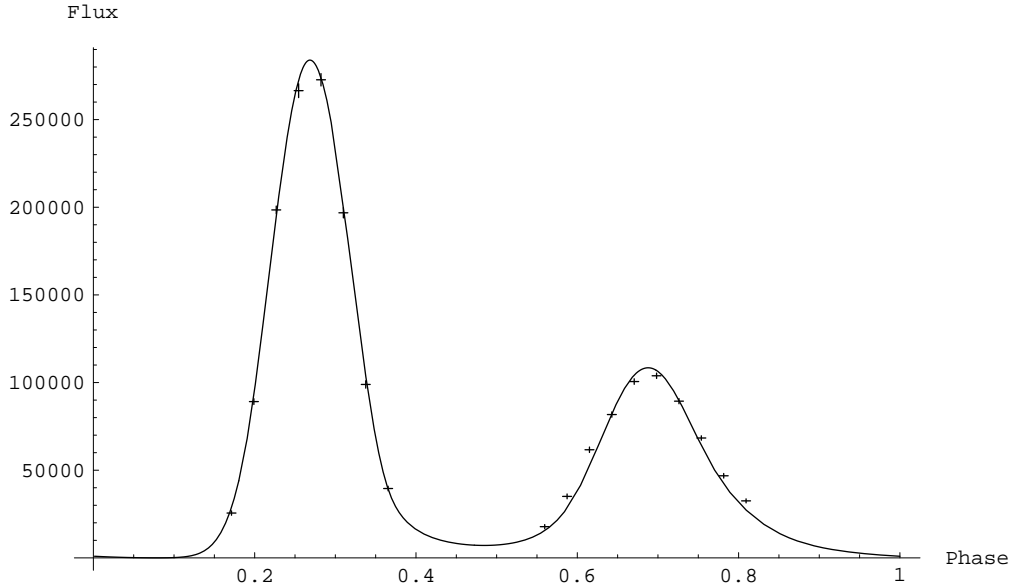


Fig. 5. Fitting the stroboscopic phase light curve to¹³ phase light curve data. Data from Fordham et al.¹³ (see Figure 3) convolved with the chopper window function are shown as a smooth curve. Corresponding stroboscopic fluxes together with flux errorbars, as given by IRAF/DAOPHOT, are shown as crosses. In finding the fit only the absolute phase and magnitude shift are considered as free parameters.